Talanta 195 (2019) 662–667

Contents lists available at ScienceDirect

Talanta

journal homepage: www.elsevier.com/locate/talanta

Qualitative and quantitative analysis of counterfeit fluconazole capsules: A non-invasive approach using NIR spectroscopy and chemometrics

O.Ye. Rodionova[a,b,*], A.V. Titova[a], N.A. Demkin[a], K.S. Balyklova[a,c], A.L. Pomerantsev[b]

[a] Information and Methodological Center for Expertise, Stocktaking and Analysis of Circulation of Medical Products, Roszdravnadzor, Slavyanskay sq., 4–1, 109074 Moscow, Russia

[b] N.N.Semenov Institute of Chemical Physics RAS, Kosygin 4, 119991 Moscow, Russia

[c] I.M. Sechenov First Moscow State Medical University, 2-4 Bolshaya Pirogovskaya Str., 2-4, 119991 Moscow, Russia

ARTICLE INFO

Keywords:
NIR spectroscopy
Counterfeit medicine
Non-invasive measurements
Fluconazole
Chemometric analysis

ABSTRACT

The ultimate goal of the study is to present a method of authentication of hard-shell capsules of medicines packed in polyvinylchloride (PVC) blisters without damaging the primary packaging. This is done by collecting NIR spectra in a non-invasive mode and subsequent analysis of measurements by a one-class classification procedure. The first part of the study demonstrates that NIR spectra collected through a PVC blister and capsule shell do carry information about the medication itself. Firstly, this is done by visual inspection of spectra of the sample, its interfering layers and main pharmaceutical ingredients. Secondly, three regression models for quantification of active pharmaceutical ingredient (API) are built. The possibility of calibration and prediction of API through several nuisance layers using NIR spectroscopy is demonstrated.

In order to solve the authentication problem the data driven soft Independent modeling of class analogies method is applied to the collected NIR spectra. The constructed model is validated using laboratory prepared mixtures. Afterwards, the model was applied to real counterfeited samples. Capsules of fluconazole are used for demonstration of the proposed approach."

1. Introduction

Revealing of counterfeit medicines is a complex and multifaceted problem. There is no single approach that is universally applicable to all drugs or is capable to address all aspects of detection [1]. Numerous testing technologies, physical and chemical, are designed to provide evidence that a product is counterfeit [2–8]. In some cases, simple visual analysis can identify a fake, in other cases this is done by the analysis of a drug's compliance to its specification or to the compendia tests. The most difficult to detect are so called 'high quality' fakes which composition is close to the genuine medicines. They are produced with violation of technological regulations, or applying low-quality ingredients [9]. Now, the World Health Organization (WHO) uses the term SF (substandard and falsified) medical products [10] for characterization of all types of counterfeit and low-quality medicines. Various qualitative analytical methods and identification tests are used for the confirmation of a certain chemical entity. However, as mentioned by the European medicines agency (EMEA), in the analysis of medical products a wider concept is used implying that qualitative tests may also include differentiation between different qualities of one chemical entity, such as polymorphs, degree of cristallinity, particle size, and etc. [11].

A very popular analytical technique is Near Infrared (NIR) spectroscopy which has been described in the European Pharmacopoeia since 1997. The principles of the NIR analysis differ from the conventional analytical methods, such as Gas chromatography (GC), or high performance liquid chromatography (HPLC), which are traditionally used in pharmaceutical analysis. For the interpretation of the NIR spectra additional chemometric analysis is usually required, giving rise to an extended term – the NIR based analysis [12]. In this concept, the NIR based analysis means application of the NIR spectroscopy together with an appropriately established chemometric technique. Among the NIR merits are the ability to conduct rapid measurements with minimal, or no sample preparations [13], as well as informativeness of the NIR spectra. The NIR signal penetrates into a sample for several millimeters and it carries information about the chemical composition, as well as about the particle sizes, the degree of cristallinity, the moisture content, polymorphs, etc. [14–16]. Moreover, the NIR based analysis implies

* Corresponding author at: N.N.Semenov Institute of Chemical Physics RAS, Kosygin 4, 119991, Moscow, Russia.
E-mail addresses: oksana@chph.ras.ru (O.Y. Rodionova), titova1701@yandex.ru (A.V. Titova), nirlab@yandex.ru (N.A. Demkin), vedeteks@yandex.ru (K.S. Balyklova), forecast@chph.ras.ru (A.L. Pomerantsev).

https://doi.org/10.1016/j.talanta.2018.11.088
Received 18 September 2018; Received in revised form 20 November 2018; Accepted 23 November 2018
Available online 29 November 2018
0039-9140/ © 2018 Elsevier B.V. All rights reserved.

This article is protected by the copyright law. You may copy and distribute this article for your personal use only. Other uses are only allowed with written permission by the copyright holder.

consideration of a medicine as a whole object, in which the complex composition of active pharmaceutical ingredients (APIs), excipients, and manufacturing conditions are taken into account. This is an important issue in counterfeit drug detection. When a suspicious sample is detected in a drugstore, or in a hospital, full information regarding the product can be ordinary found on its package. Therefore, the anti-counterfeiting task is to determine whether the suspicious remedy is what it is claimed to be. This is an authentication problem and it is wider than classical qualitative analytical testing.

The rapid spectroscopic technique offers an opportunity for massive monitoring of drugs at the end points of their circulation. At the same time, for economic reasons, it is required that this monitoring can be carried out in a non-invasive manner, through the primary packaging – blisters, capsules, etc. In this case, an approbated sample can be returned to circulation. In our previous works [9,17] it has been shown that the NIR based analysis in the diffuse reflection mode ensures this possibility for a wide range of tablets packed in blisters. In this paper we consider a more complex object, namely the blister packaged capsules.

A capsule is a widely used solid dosage form intended for oral administration. The hard-shell gelatin capsules are normally used for dry powdered ingredients, or pellets. Shells of this type consist of two parts: a capsule body and a cup. Basic gelatin shells are made of mixtures of gelatin and water; they are transparent, colorless, and tasteless. Optionally, the shells could be colored, or opacified, to provide protection. Often a set of capsules is packed into a polyvinylchloride (PVC) blister. Thus, the target to be analyzed is a drug inside the capsule placed under PVC film. These two external layers (gelatin and PVC) generate extraneous NIR signals which distort the spectrum of the target drug. We demonstrate that, in spite of these obstacles, the quantification and authentication of the target can be performed with a proper accuracy in a non-invasive manner.

An additional aspect of this research is that the concentration of the active pharmaceutical ingredient (API) is calibrated and predicted with a practically sufficient accuracy. In our opinion, it is the first time when API is assessed through several nuisance layers using NIR spectroscopy. In general, we prefer using a qualitative approach for drug authentication, because a sole API quantification is not sufficient to reveal 'high-quality' counterfeits' [9]. However, there is a strong belief that such analytical problem as the determination of a mixture component in a sample hidden under a multilayer cover has particular value.

In summary, the goal of this study is to present a non-invasive NIR-based method for the quantitative and qualitative analysis of medicines in hard-shell capsules packed in PVC blisters. The object under study is Fluconazole [18,19], which is presented in both genuine and counterfeited samples. The calculations were conducted using Chemometrics add-in for Excel [20] and freely available GUI tool "DD-SIMCA" [21].

2. Materials and methods

2.1. Intact capsules

Fluconazole (international nonproprietary name) is the synthetic triazole with antifungal activity. The capsule with a total mass of 350 mg contains 150 mg of API, 147.5 mg of lactose monohydrate, and minor quantities of corn starch, magnesium stearate, silicon dioxide, and sodium lauryl sulfate. The opaque capsule's shell is made of gelatin with an addition of 2% of titanium dioxide.

2.2. API and excipients

Fluconazole substance (chemical name: 2-(2,4-Difluorophenyl)-1,3-bis(1*H*-1,2,4-triazol-1-yl)propan-2-ol) was provided by the manufacturer of the fluconazole capsules analyzed in this study. It is a white crystalline powder, which is slightly soluble in water, freely soluble in methanol, and soluble in acetone. Lactose monohydrate 80 MESH (DFE Pharma, the Netherlands) was used to compose the designed samples.

Table 1
Designed samples.

Sample #	API mass (mg)	Calculated API fraction (% w/w)	Referenced API fraction (% w/w) + STD
1	200	49.00	50.06 ± 0.49
2	150	41.77	41.15 ± 0.79
3[*)]	125	34.75	34.28 ± 0.23
4	100	27.84	28.54 ± 0.82
5	75	20.84	20.85 ± 0.06
6[a]	50	13.92	13.28 ± 0.57
7	25	6.91	6.60 ± 0.14
8	0	0.00	0.00

[a] Used in the test set for quantitative analysis.

2.3. Designed samples

The genuine capsules from five batches are used in the experiment. Their content is extracted into a bulk, which portions are diluted by various amounts of lactose (see Table 1). Sample #1 has an increased API concentration; it is composed of the capsule contents with extra addition of API. Sample #2 corresponds to the dosage form. Sample #8 is composed of pure lactose monohydrate. In such a manner, a set of calibration samples with different concentrations of API was made. The designed API concentrations are confirmed using the UV spectrometry test.

2.4. Data sets

In order to study the possibilities of the non-invasive analysis of capsules, five data sets are used. Three datasets are composed of the NIR spectra acquired using the mixtures that were specially designed (Table 1).

Dataset 1 consists of the bulk mixtures (powder). Dataset 2 includes capsules filled with these mixtures. For this purpose, the capsule shells of the genuine medicines are hollowed out and filled up. Each mixture is placed into three capsules in order to account for a possible variation in capsules. Dataset 3 comprises the capsules from dataset 2 placed into PVC blisters obtained from the genuine packages.

Two additional data sets represent the real-world objects. Dataset 4 consists of genuine capsules from 5 batches provided by the manufacturer. Dataset 5 includes suspicious drugs samples, which were seized from a drugstore as the package appearance aroused suspicion. We have 2 boxes that are labeled as the abovementioned genuine medicines.

A summary of the data collection, and the way the datasets are analyzed are presented in Fig. 1.

2.5. Reference method

The reference concentration of Fluconazole in the designed samples (datasets 1–3) was determined using the UV-spectroscopy method [22]. The diode-array spectrophotometer SPECORD S600 (Analytik Jena, Germany) with the 1 cm quartz cells was applied. Absorbance was measured at 261 nm using 0.1 M HCl as solvent for the preparation of the standard and sample solutions. Measurements were conducted in triplicates. The obtained concentrations are given in column 'Referenced fraction' in Table 1, together with the standard deviation value (STD) for each concentration.

2.6. NIR spectra acquisition

All spectra are acquired in the diffuse reflection mode using a handheld fiber probe (FP) in the spectral range of 12500–4000 cm^{-1} with resolution of 8 cm^{-1}. The FT-NIR spectrometer (MPA by Bruker Optics, Germany) was used. Measurements of the mixtures (dataset 1)

This article is protected by the copyright law. You may copy and distribute this article for your personal use only. Other uses are only allowed with written permission by the copyright holder.

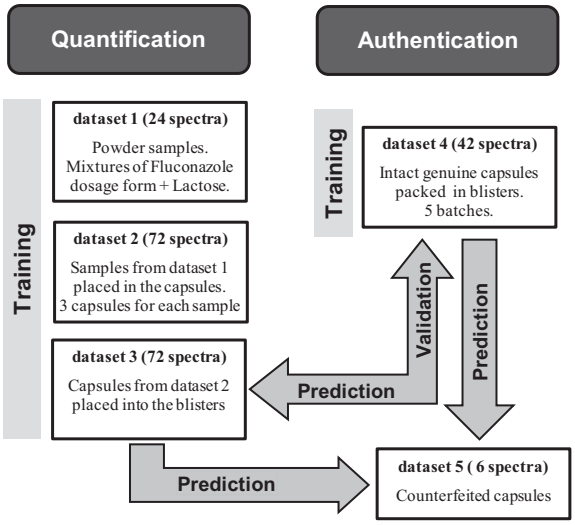

Fig. 1. Summary of datasets used for quantification and authentication.

are conducted by immersing FP directly into a glass vial. Measurements of the packaged samples are performed directly through the capsules (dataset 2), or through the combination of a PVC blister and a capsule (dataset 3). Measurements of the real-world intact capsules (dataset 4 and 5) are taken in the same manner as for dataset 3. All measurements of capsules are conducted through the capsule body.

NIR measurements of each experimental unit – a vial, a capsule, and a spot on a blister – were conducted three times. At every attempt the unit position was slightly changed; see the graphical abstract as an illustration. In the result, the following number of the NIR spectra was collected. For datasets 1 it is $8 \times 3 = 24$; for datasets 2 and 3 they are $8 \times 3 \times 3 = 72$; for dataset 4 it is $2 \times 3 \times 2 + 4 \times 3 \times 2 = 42$, and for dataset 5 it is $2 \times 3 = 6$.

For chemometric analysis an informative spectral region of 9000–4150 cm^{-1} is used. The range between 12500 and 9000 cm^{-1} is considered to be little informative and the range of 4150–4000 cm^{-1} is excluded due to the low reproducibility of the FP measurements [23]. The obtained NIR spectra are pretreated using the Standard Normal Variate (SNV) method [24].

It should be mentioned that here we come across the so-called 'high quality' counterfeiting [9] as the NIR spectra of the genuine and counterfeited samples are very similar (see Fig. 2). Nevertheless, we will present a convincing affirmation that the suspicious samples are falsified ones.

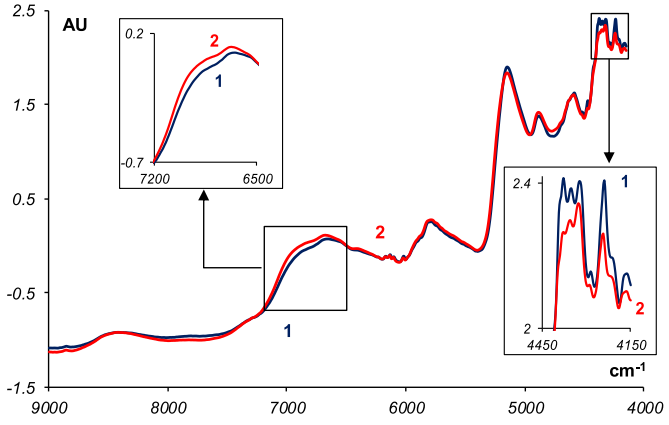

Fig. 2. Normalized spectra. (1, black) intact genuine capsule measured through PVC; (2, red) intact counterfeited capsule measured through PVC.

2.7. Chemometrics methods

For the data analysis two popular chemometric techniques are employed.

Partial least squares regression (PLS) is the method used for the quantitative analysis. Its detailed description may be found elsewhere [24]. It relates the data matrix of predictors **X** with the vector of responses **y**. In our case, matrix **X** is the collection of the spectra, and vector **y** comprises the concentration values given in Table 1. This method predicts the concentration $\hat{\mathbf{y}}$, which better corresponds to a given spectrum **x**. The PLS model can use a different number of Latent Variables (LVs), which represent the model complexity. The optimal number of LVs is selected comparing the root mean squared errors of calibration (RMSEC), validation (RMSEP), and/or cross validation (RMSECV) [25]. Formula for calculations is as follows

$$RMSE = \sqrt{\frac{1}{I}\sum_{i=1}^{I}(\hat{y}_i - y_i)}, \quad (1)$$

where I is the number of samples in the training (RMSEC) or in the test (RMSEP) sets, and $\hat{y}_i$ are the values calculated by the PLS model for the training or test samples. The RMSECV value is calculated in a similar way [20,24].

The qualitative data analysis (authentication [26]) is conducted using the SIMCA method [27] in its modern version known as Data Driven SIMCA (DD-SIMCA) [28], which has an ability to calculate the errors of misclassification theoretically [29]. SIMCA is primarily focused on the description of a particular, target class [26], which is presented by a representative set of the genuine samples. Other objects, which are not members of the target class, are considered as aliens.

The SIMCA model is developed using principal component analysis (PCA) [30]

$$\mathbf{X} = \mathbf{T}\mathbf{P}^t + \mathbf{E} \quad (2)$$

applied to the training matrix **X**. The PCA results are used for calculation of two distances for each object. They are the score distance, H_i, and the orthogonal distance, Q_i:

$$H_i = \mathbf{t}_i^t(\mathbf{T}^t\mathbf{T})^{-1}\mathbf{t}_i, \quad Q_i = \sum_{j=1}^{J} e_{ij}^2 \quad (3)$$

These distances are used to establish two tolerance limits: the acceptance area for a given significance level α, and the outliers area that depends on a given outliers level γ. The SIMCA results can be presented using a two-dimensional plot [28], where each sample is shown in the coordinates $\ln(1 + H_i/H_0)$ vs $\ln(1 + Q_i/Q_0)$, together with the threshold curves, which delineate the regular, extreme, and outlier samples.

To assess the quality of authentication, terms 'sensitivity' and 'specificity' are used [31]. Sensitivity is the percentage of samples from the target class which are properly attributed as members of this class. Specificity is the percentage of alien objects which are properly attributed as non-members of the target class.

3. Results and discussion

3.1. Non-invasive measurements

NIR data are acquired for complex multi-layers objects. Each spectrum is a combination of two spectra of interfering layers, and a spectrum of the multi-component powder. Fig. 3 illustrates the appearance of the resulting spectrum (curve 1). The first layer is the PVC film (curve 2), which has strong absorption bands around 5800 cm^{-1} and in the area of 4450–4000 cm^{-1} (combination bands close to the IR range). These bands partly mask the spectrum of the dosage form (curve 1). In other regions, the PVC film is almost transparent to the NIR irradiation. The highest bands, which are visible in the resulting spectra,

This article is protected by the copyright law. You may copy and distribute this article for your personal use only. Other uses are only allowed with written permission by the copyright holder.

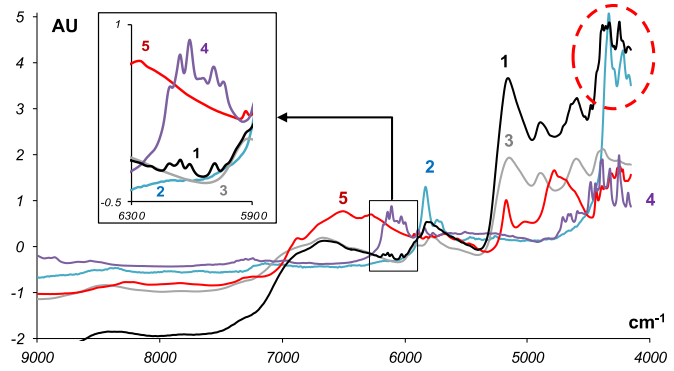

Fig. 3. Normalized spectra. (1, black) intact capsule through PVC; (2, blue) PVC blister; (3, grey) empty capsule; (4, purple) API, (5, red) lactose;.

correspond to the capsule shell (curve 3). However, there are regions where the API bands (curve 4) are seen, i.e. in the region of 4500–4300 cm^{-1} (marked by the red oval), and around 6300–5900 cm^{-1} (see insert). Curve 5 represents the spectrum of lactose monohydrate. This excipient comprises half of the contents of the capsule, so it strong impacts the resulting spectrum. Thus, we can conclude that the obtained spectrum carries information about the interfering layers and about the capsule contents, i.e. the medicine itself. Previously, this problem was partly investigated in [32].

3.2. Quantification

Several PLS models are built for the quantitative determination of API. Data sets 1–3 are used for these purposes (see Table 1). The results of calibration are shown in Table 2.

The RMSEP values are calculated using samples #3 and #6 (see Table 1), which are included in the test set. Correspondingly, RMSEC is calculated without those samples. In Table 2, column $RMSECV_1$ represents the calibration errors obtained using the leave-one-out (LOO) cross-validation. At the same time, as we have several measurements for each concentration point, all these spectra should be left out at a cross-validation step for more reliable estimates. $RMSECV_2$ provides greater values than $RMSEV_1$ mainly due to the fact that calculations leave out points at the edges of the calibration range.

The model for dataset 1 is the simplest one. It seems that one LV should be enough, but the second LV accounts for some nonlinearity, which exists in the data, so the second component can improve calibration accuracy.

Calibration of dataset 2 is hindered by the presence of the capsule shell, the spectrum of which influences the results greatly. The increase of the LV number does not improve model accuracy essentially. Since the capsule shell is made of gelatin that contains about 13–15% of water, the region between 5300 cm^{-1}–4900 cm^{-1}, which corresponds to the combination of stretching and deformation of the O–H group in water, is removed. The calibration based on the reduced spectral range (Table 2, dataset 2) and three LVs provide better results. For calibration of dataset 3, the same reduced spectral range is applied. The model, where data acquisition is conducted through PVC and capsule shell, demonstrates practically sufficient accuracy (see Fig. 4).

The PLS calibration model, which was obtained for dataset 3, is used

Table 2
Characteristics of the PLS models. RMSE is given in % w/w.

Data set	LVs	RMSEC	$RMSECV_1$	$RMSECV_2$	RMSEP
Dataset 1	2	1.43	1.64	2.88	1.22
Dataset 2	3	1.47	1.62	2.18	1.76
Dataset 3	3	1.69	1.90	2.43	1.72

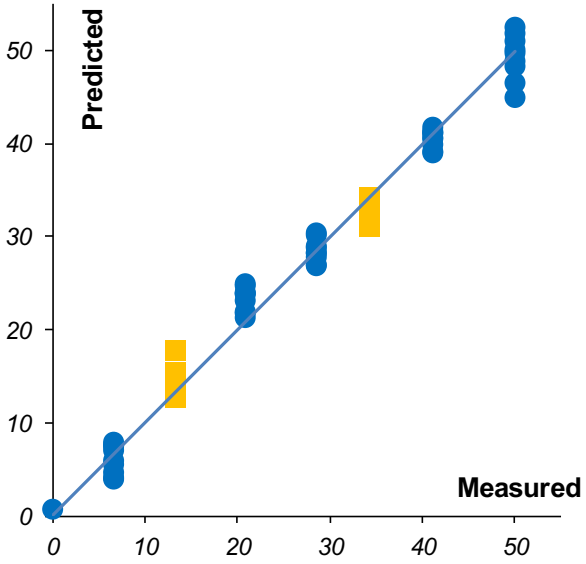

Fig. 4. Predicted vs measured (% w/w) by the PLS model for dataset 3 with three LVs. Training samples are shown by the blue diamonds, the test samples are presented by the yellow squares (For interpretation of the references to color in this figure legend, the reader is referred to the web version of this article.).

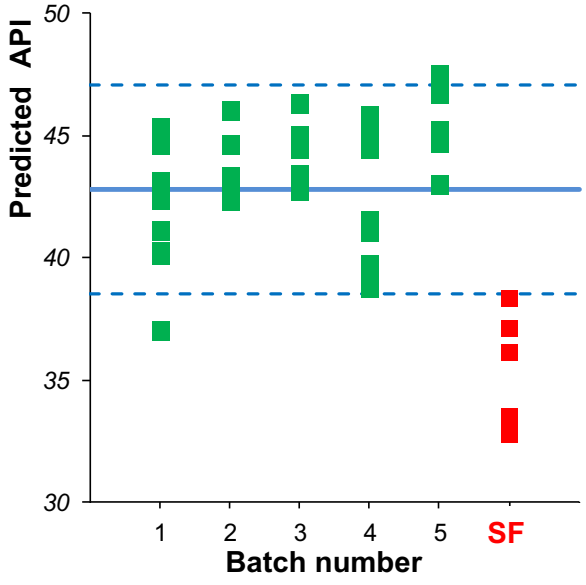

Fig. 5. Prediction the fluconazole concentrations (% w/w) for dataset 4 (green squares) and dataset 5 (red squares) (For interpretation of the references to color in this figure legend, the reader is referred to the web version of this article.).

for prediction of the fluconazole concentration in the real-world samples. It is applied to dataset 4, which consists of the genuine samples (5 batches) provided by manufacturer, and to dataset 5, which includes 6 suspicious samples. The results are shown in Fig. 5.

It should be noted that the indication on the package that fluconazole mass is 150 mg (42.86% w/w, the blue line in Fig. 5) does not mean that each capsule contains this amount of API exactly. The pharmacopoeia rules allow variation of the API mass up to 10%, and these admissible levels are represented by the blue dashed lines in Fig. 5. If a sample is located between these dashed lines, it is considered acceptable. We can see that almost all genuine samples (dataset 4), which are represented by the green squares, passed this test. The suspects (the red squares) have API concentrations which are located

This article is protected by the copyright law. You may copy and distribute this article for your personal use only. Other uses are only allowed with written permission by the copyright holder.

beyond the lower limit. Therefore, they are SFs indeed.

It is interesting to compare the obtained RMSE values (Table 2) with the admissible levels, which are 42.80 ± 4.28 (% w/w). Considering that this interval corresponds to the doubled sigma (95% confidence), we obtain RMSEA = 2.14 (% w/w), where RMSEA is the root mean squared error in API concentration allowed by the pharmacopoeia rules. From Table 2, we can extract RMSE values for dataset 3, which are $RMSECV_2$ = 2.43, and RMSEP = 1.72 (% w/w). This leads to the conclusion that the accuracy obtained in the non-invasive determination of fluconazole is compatible with the admissible level of the API variation in the drug. We consider this accuracy as practically sufficient.

We demonstrated, for the first time, that non-invasive NIR measurements conducted through several hindering layers can be utilized for a quantitative determination of a component in a hidden mixture. However, we do not recommend this method, or any other quantitative approach, as the ultimate technique to reveal SFs. In our opinion, a qualitative (authentication) approach, which accounts for all features of a sample, is more suitable for this purpose.

3.3. Authentication

The SIMCA model employed for authentication is developed using dataset 4. This set consists of forty two spectra used for the model training. The dataset 3 comprises the test set used for model optimization, which is based on the following rule. A sample with a proper API concentration (Table 1, sample # 2) should be accepted, but the samples with lower and higher API concentrations should be rejected. In another words, it is supposed that the target class combines dataset 4 and spectra for sample #2 from dataset 3.

It is hard to foresee what kind of falsification can be encountered in the course of routine drug monitoring. Very often an increased moisture content signals counterfeiting. Therefore, the entire informative spectral region of 9000–4150 cm^{-1} is used for the modeling.

The SIMCA model, developed for 4 PCs at $\alpha = 0.01$ and $\gamma = 0.01$, is shown in Fig. 6. The left plot (a) demonstrates the results obtained for the training set. The green curve delineates the acceptance area. It can be seen that all genuine samples (the green dots) except one are accepted as members of the target class. The extreme sample (the yellow diamond) does not compromise the model, because the expected sensitivity of 99% is very close to the obtained sensitivity of 98%.

The right plot (b) shows the prediction results obtained for dataset 3 (various blue marks) and dataset 5 (the red squares). The repeated measurements of sample #2, which is a member of the target class, are represented by the light blue dots that are located inside the acceptance area (below the green curve). This means that the model sensitivity at prediction is 100%. Other samples from dataset 3 are located beyond the acceptance area and thus they are properly classified as the non-members, so the model specificity is equal to 100%.

A proper allocation of the alien samples can also be mentioned – the smaller the API concentration is, the farther from the acceptance area the sample is located. Samples #1, which have increased API concentrations, are also located outside of the acceptance area, but rather close to its border.

An approach, when a SIMCA model is developed and validated using only target samples, is called rigorous. In the absence of alien objects it is impossible to assess model specificity. In case the SIMCA model is based on dataset 4 alone, three PCs are enough: all training samples are properly classified and sensitivity is equal to 100%. However, in this case, in prediction, the sample #1 spectra are wrongly classified as the target class members, and the model specificity equals 94%.

In case of the compliant approach [33], information regarding the alien samples is also utilized for the model development. In our case, dataset 3 is used as a source of extraneous samples. To increase the model specificity four PCs are selected. However, one object from the training set becomes an extreme and the model sensitivity is decreased to 97%.

The trade-off between model sensitivity and specificity is a common case in qualitative modeling. The ultimate decision should be made by an expert who has to determine what result is more admissible: to reject several samples from the target class (the type I error), or to accept some alien objects as the target members (the type II error).

As soon as a SIMCA model is developed, it can be used for routine authentication. Applying this model to the spectra acquired from the suspicious samples (data set 5), we can conclude that these samples are not authentic as they are located far from the acceptance area (Fig. 6b, red squares). Together with the results obtained from the quantitative model (Fig. 5) we can assert that samples from dataset 5 are counterfeits.

4. Conclusions

Despite of the fact that we analyze complex multi-layers objects, our

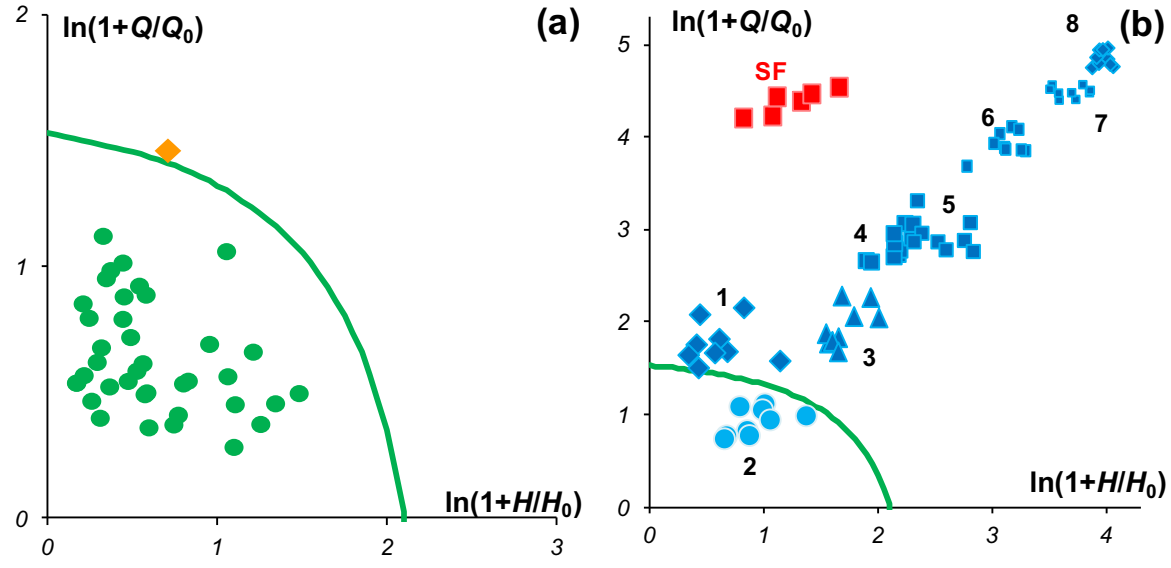

Fig. 6. Acceptance plots for SIMCA model. (a) Training, (b) Prediction. Number in the plot (b) correspond to the sample shown in Table 1 (For interpretation of the references to color in this figure legend, the reader is referred to the web version of this article.).

This article is protected by the copyright law. You may copy and distribute this article for your personal use only. Other uses are only allowed with written permission by the copyright holder.

study shows that it is possible to extract important information about the medicine, which is located underneath the layers. The acquired spectra really carry information regarding all elements of the remedy. While two outer layers, the PVC-film and the shells of the capsules, are considered as interfering layers, they are an inherent part of a dosage form. Therefore, any irregularities regarding the packaging layer, the capsule shell, or the capsule contents, lead to changes in the acquired spectrum and, in this way, signal that the sample is counterfeit.

The presented authentication procedure demonstrates the ability of proper allocation of the target objects and detection of the SF-objects of various nature, even when falsified samples are very similar to the genuine ones. The results of the PLS-regression provide additional confirmation that suspicious samples are counterfeits. It should be emphasized that the proper concentration of API in a dosage form does not guarantee that the medicine is a genuine one. In our study [9], we have come across falsified tablets that had a proper API concentration, but were produced by an illegal manufacturer. Therefore, the calibration model developed for quantification of the API concentration in capsules measured in a non-invasive mode can be used as an additional, but not sole technique of authentication.

In a general, there is no need to build a regression model. At the same time, this procedure helps to assess the API concentration of each capsule in a way that is much easier than standard laboratory tests, where, as a rule, the contents of several capsules (e.g. an assay of fluconazole needs 20 capsules) should be mixed together and analyzed. This feature could help to reveal substandard samples which, for example, demonstrate heterogeneity of dosing.

The availability of a rapid and non-invasive procedure for authentication of certain types of medicines is very important. It provides possibilities to test many samples in mobile laboratories and, thus, to assure the quality of medicines in drugstores and hospitals. It also greatly simplifies work in testing labs.

Acknowledgement

ALP and OYR acknowledge a partial support within the Russian State Assignment, Russia AAAA-A18-118020690203-8, №0082-2018-0005.

References

[1] R. Martino, M. Malet-Martino, V. Gilard, S. Balayssac, Counterfeit drugs: analytical techniques for their identification, Anal. Bioanal. Chem. 398 (1) (2010) 77–92, https://doi.org/10.1007/s00216-010-3748-y.

[2] U. Bussy, C. Thibaudeau, F. Thomas, J.-R. Desmurs, E. Jamin, G.S. Remaud, V. Silvestre, S. Akoka, Isotopic finger-printing of active pharmaceutical ingredients by 13C NMR and polarization transfer techniques as a tool to fight against counterfeiting, Talanta 85 (4) (2011) 1909–1914, https://doi.org/10.1016/j.talanta.2011.07.022.

[3] E. Dinc, D. Baleanu, G. Ioele, M. De Luca, G. Ragno, Multivariate analysis of paracetamol, propiphenazone, caffeine and thiamine in quaternary mixtures by PCR, PLS and ANN calibrations applied on wavelet transform data, J. Pharm. Biomed. Anal. 48 (5) (2008) 1471–1475, https://doi.org/10.1016/j.jpba.2008.09.035.

[4] D. Custers, B. Krakowska, J.O. De Beer, P. Courselle, M. Daszykowski, S. Apers, E. Deconinck, Chromatographic impurity fingerprinting of genuine and counterfeit Cialis® as a means to compare the discriminating ability of PDA and MS detection, Talanta 146 (1) (2016) 540–548, https://doi.org/10.1016/j.talanta.2015.09.029.

[5] Y. Roggo, K. Degardin, P. Margot, Identification of pharmaceutical tablets by Raman spectroscopy and chemometrics, Talanta 81 (3) (2010) 988–995, https://doi.org/10.1016/j.talanta.2010.01.046.

[6] J. Dubois, J.-C. Wolff, J.K. Warrack, J. Schoppelrei, E.N. Lewis, NIR chemical imaging for counterfeit pharmaceutical products analysis, Spectroscopy 22 (2) (2007) 40–50.

[7] R.W. Jähnke, Counterfeit medicines and the GPHF-Minilab for rapid drug quality verification, Pharm. Ind. 66 (10) (2004) 1187–1193.

[8] M.T. Koesdjojo, Y. Wu, A. Boonloed, E.M. Dunfield, V.T. Remcho, Low-cost, high-speed identification of counterfeit antimalarial drugs on paper, Talanta 130 (2014) 122–127, https://doi.org/10.1016/j.talanta.2014.05.050.

[9] O.Ye Rodionova, K.S. Balyklova, A.V. Titova, A.L. Pomerantsev, Application of NIR spectroscopy and chemometrics for revealing of the 'high quality fakes' among the medicines, Forensic Chem. 8 (2018) 82–89, https://doi.org/10.1016/j.forc.2018.02.004.

[10] Definitions of Substandard and Falsified (SF) Medical Products. ⟨http://www.who.int/medicines/regulation/ssffc/definitions/en/⟩, (Accessed 3 September 2018).

[11] Guideline on the use of near infrared spectroscopy by the pharmaceutical industry and the data requirements for new submissions and variations. ⟨http://www.ema.europa.eu/docs/en_GB/document_library/Scientific_guideline/2014/06/WC500167967.pdf⟩, (Accessed 3 September 2018).

[12] O.Ye Rodionova, A.L. Pomerantsev, NIR-based approach to counterfeit-drug detection, Trends Anal. Chem. 29 (8) (2010) 795–803, https://doi.org/10.1016/j.trac.2010.05.004.

[13] P. Chalus, Y. Roggo, S. Walter, M. Ulmschneider, Near-infrared determination of active substance content in intact low-dosage tablets, Talanta 66 (5) (2005) 1294–1302, https://doi.org/10.1016/j.talanta.2005.01.051.

[14] L. Rigoni, S. Venti, M. Bevilacqua, R. Bucci, A.D. Magrì, A.L. Magrì, F. Marini, Quantification of the enantiomeric excess of two APIs by means of near infrared spectroscopy and chemometrics, Chemom. Intell. Lab. Syst. 133 (2014) 149–156, https://doi.org/10.1016/j.chemolab.2014.02.004.

[15] S.J. Bai, M. Rani, R. Suryanarayanan, J.F. Carpenter, R. Nayar, M.C. Manning, Quantification of glycine crystallinity by near-infrared (NIR) spectroscopy, J. Pharm. Sci. 93 (10) (2004) 2439–2447, https://doi.org/10.1002/jps.20153.

[16] J. Mantanus, E. Ziémons, P. Lebrun, E. Rozet, R. Klinkenberg, B. Streel, B. Evrard, P. Hubert, Moisture content determination of pharmaceutical pellets by near infrared spectroscopy: method development and validation, Anal. Chim. Acta 642 (2009) 186–192, https://doi.org/10.1016/j.aca.2008.12.031.

[17] Y.V. Zontov, K.S. Balyklova, A.V. Titova, O.Ye Rodionova, A.L. Pomerantsev, Chemometric aided NIR portable instrument for rapid assessment of medicine quality, J. Pharm. Biomed. Anal. 131 (2016) 87–93, https://doi.org/10.1016/j.jpba.2016.08.008.

[18] The International Pharmacopoeia – Eighth Edition. ⟨http://apps.who.int/phint/2018/index.html#d/b.6.2.2.58⟩, (Accessed 14 November 2018).

[19] H. Bourichi, Y. Brik, P. Hubert, Y. Cherrah, A. Bouklouze, Solid-state characterization and impurities determination of fluconazol generic products marketed in Morocco, J. Pharm. Anal. 2 (6) (2012) 412–421, https://doi.org/10.1016/j.jpha.2012.07.010.

[20] A.L. Pomerantsev, Chemometrics in Excel, John Wiley & Sons, Hoboken, NJ, 2014, https://doi.org/10.1002/9781118873212.

[21] Y.V. Zontov, O. Ye, Rodionova, S.V. Kucheryavskiy, A.L. Pomerantsev, DD-SIMCA – a MATLAB GUI tool for data driven SIMCA approach, Chemom. Intell. Lab. Syst. 167 (2017) 23–28, https://doi.org/10.1016/j.chemolab.2017.05.010.

[22] P. Sadasivudu, N. Shastri, M. Sadanandam, Development and validation of RP-HPLC and UV methods of analysis for fluconazole in pharmaceutical solid dosage forms, Int. J. ChemTech Res. 1 (4) (2009) 1131–1136.

[23] O.Ye Rodionova, K.S. Balyklova, A.V. Titova, A.L. Pomerantsev, The influence of fiber-probe accessories application on the results of near-infrared (NIR) measurements, Appl. Spectrosc. 67 (12) (2013) 1401–1407, https://doi.org/10.1366/13-07134.

[24] T. Næs, T. Isaksson, T. Fearn, T. Davies, A User-Friendly Guide to Multivariate Calibration and Classification, NIR Publications, Chichester, UK, 2002.

[25] K. Esbensen, P. Geladi, Principles of Proper Validation: use and abuse of re-sampling for validation, J. Chemom. 24 (2010) 168–187, https://doi.org/10.1002/cem.1310.

[26] O.Ye Rodionova, A.V. Titova, A.L. Pomerantsev, Discriminant analysis is an inappropriate method of authentication, Trends Anal. Chem. 78 (4) (2016) 17–22, https://doi.org/10.1016/j.trac.2016.01.010.

[27] S. Wold, M. Sjostrom, SIMCA: a method for analyzing chemical data in terms of similarity and analogy, in: B.R. Kowalski (Ed.), In Chemometrics: Theory and Application, ACS Symposium Series, American Chemical Society, Washington D.C, 1977, pp. 243–282.

[28] A.L. Pomerantsev, O.Y. Rodionova, Concept and role of extreme objects in PCA/SIMCA, J. Chemom. 28 (2014) 429–438, https://doi.org/10.1002/cem.2506.

[29] A.L. Pomerantsev, O.Y. Rodionova, On the type II error in SIMCA method, J. Chemom. 28 (2014) 518–522, https://doi.org/10.1002/cem.2610.

[30] H. Martens, T. Naes, Multivariate Calibration, Wiley, New York, 1998.

[31] S.N. Deming, Y. Michotte, D.L. Massart, L. Kaufman, B.G.M. Vandeginste, Chemometrics: A Textbook, Elsevier, Amsterdam, 1988.

[32] A.L. Pomerantsev, O.Ye Rodionova, A.N. Skvortsov, Diffuse reflectance spectroscopy of hidden objects, part I: interpretation of the reflection-absorption-scattering fractions in near-infrared (NIR) spectra of polyethylene films, Appl. Spectrosc. 71 (8) (2017) 1760–1772, https://doi.org/10.1177/0003702817694182.

[33] O.Ye Rodionova, P. Oliveri, A.L. Pomerantsev, Rigorous and compliant approaches to one-class classification, Chemom. Intell. Lab. Syst. 159 (2016) 89–96, https://doi.org/10.1016/j.chemolab.2016.10.002.

This article is protected by the copyright law. You may copy and distribute this article for your personal use only. Other uses are only allowed with written permission by the copyright holder.